Simultaneous Measurement of Temperature and Strain by Cascaded Fiber Bragg Grating-Silicon Fabry-Perot Interferometer Sensor

Hasanur R. Chowdhury, Xiaoli Wang, and Ming Han*
Michigan State University, East Lansing, Michigan 48823, USA

Abstract. We report a fiber-optic sensor configuration with a cascaded fiber Bragg grating (FBG) and a silicon Fabry-Perot interferometer (FPI) for simultaneous measurement of temperature and strain. The sensor is composed of a 5 mm FBG on a single mode fiber and a 100 μm thick silicon FPI attached to the tip of the optical fiber. The FBG is surface mounted on the host structure, while the FPI tip is suspended. Due to the stress-free, cantilever configuration, the silicon FPI is insensitive to strain, but sensitive to temperature with a sensitivity much higher than the FBG due to the large thermo-optic coefficient of silicon. The sensor is tested from room temperature to 100 °C with varying strain up to ~150 με. The silicon FPI provides high temperature sensitivity of 89 pm/°C unaffected by strain. Since the FBG is attached to the host structure, it is affected by both thermal and mechanical strain; the sensitivity of these were experimentally obtained 32 pm/°C and 1.09 pm/με, respectively. Interrogated with a broadband light source and a high-speed spectrometer, the sensor shows temperature and strain resolutions of 1.9×10^{-3} °C and 0.042 με, respectively. Due to the small size, enhanced sensitivity, and high resolution, this cascaded FBG-FPI sensor can be used in applications where accurate measurement of temperature and strain are required.

Keywords: Fiber optic sensors, temperature, strain, Fabry-Perot interferometer, fiber Bragg grating.

*Corresponding author, E-mail: mhan@egr.msu.edu

1 Introduction

Temperature and strain are two key parameters to monitor for safety purpose, and enhancing the efficiency of many modern industries including aerospace, petroleum and mining, power plants, structural health monitoring and biomedical applications [1,2]. Conventional thermocouples along with strain gauges are used to measure these parameters; however, these have drawbacks of complex wiring, cross sensitivity, long term drift, and signal demodulation limitation [3]. Fiber optic sensors have gained popularity as an alternative to thermocouples and strain gauges due to their many unique advantages, such as small size, high accuracy, immunity to electromagnetic interference, harsh environment compatibility and multiplexing capacity [4]. But these two parameters are inter-related to each other and hence it becomes difficult to measure both simultaneously with high accuracy.

In the last few decades, many research have been conducted on multiparameter measurement using fiber optic sensors, mostly fiber Bragg grating (FBG) [5–7], Fabry-Perot interferometers (FPI) [8,9], Brillouin frequency shift [10,11] and fiber loop ringdown [12,13]. To measure multiple parameters simultaneously, we need at least two characteristic indicators (wavelengths, phase, intensity) with different sensitivities to different measurands (temperature, strain, pressure etc.). Demodulation of the measurand's value is performed by the sensitivity matrix or characteristic equations [14]. However, these methods have some limitations, such as complex fabrication process, limited sensitivity to prevent temperature crosstalk, multiplexing and interrogating several fibers etc. For example, a typical FBG has temperature and strain sensitivity as 11 pm/℃ and 1 pm/$\mu\varepsilon$, respectively, which limits its operation in harsh environment with significant fluctuations in strain/temperature. To enhance the sensitivity, many researchers have incorporated modification in the fiber by using arched/tapered core FBG sensors [15]. But most of these require complex MEMS techniques or optical fusion tapering system for fabrication, which is expensive, complex, and hard to reproduce. Tian et el. [7] has proposed a dual FBG configuration with one of the FBGs incorporated in capillary tube, where the strain sensitivity was increased to 5.46 pm/με, but the temperature sensitivity was not improved much (15.7 pm/℃). Ref [5] used a single FBG, partly bonded and partly unbonded to the host structure to discriminate strain and temperature sensitivity, but the low sensitivity issue of FBG to strain remained unanswered. In recent time, a new scheme is invented where two FPI sensors are used to form optical vernier effect [16–18] for enhanced sensitivity. Although this configuration renders well for single parameter measurement, it needs an isolation technique between the reference FP and measuring FP to minimize cross-talk for simultaneous measurement. Another prospective research is to use a configuration with cascaded FBG and FPI for simultaneous measurement of multiple parameters such as temperature and gas pressure [19], temperature and refractive index [20], temperature and magnetic field [21], and temperature and strain [22–24]. For temperature and strain measurement, the FPI typically is an air cavity fabricated with laser drilling or splicing optical fibers to both ends of a hollow glass tube. Both the FBG and FPI have similar sensitivities to strain (~1.2 pm/με) as a given strain corresponds to the same changes of the grating pitch for an FBG and of the cavity length for an FPI. Differentiating temperature and strain relies on the different responses of the FBG and the FPI to temperature. Specifically, an FBG shows a temperature sensitivity of ~11 pm/°C mainly from the thermo-optic effect of the fiber material, while an air-cavity FPI with a silica structure is insensitive to temperature due to the small thermal expansion coefficient of silica. For strain measurement in practice, the sensor including the air-cavity FPI usually needs to be bonded on the surface of a structure. The temperature sensitivity of the air cavity FPI can be greatly affected by the thermal strain of the structure. In some cases, the thermal strain may lead to a temperature sensitivity of the FPI comparable to that of the FBG, which makes the differentiation of temperature and strain difficult. As a result, many of the abovementioned works [6–13,15,17,22–24] used translation stage to stretch the fiber with forces applied at two points on the fiber for strain test to avoid the interference from thermal strain. The two-point loading can only transfer the tensile strain to the sensor but not compressive strains. Additionally, the fabrication method of the air-cavity FPIs involving laser drilling and splicing may reduce the mechanical strength of the sensor.

In this work, we report a cascaded FBG-FPI sensor for which the FPI is a small silicon pillar attached to the tip of the fiber for simultaneously measurements of temperature and strain with significantly improved temperature sensitivity and reduced crosstalk. The sensor is composed of a FBG inscribed in a single mode fiber (SMF) and a 100 μm long silicon pillar attached to the tip of the fiber functioning as an FPI. For the implementation of the sensor, the FBG is surface mounted onto the structure to measure its strain, while the FPI tip is suspended in air. The silicon FPI tip has a stress-free cantilever configuration, which makes it insensitive to strain. Due to the large thermo-optic coefficient of silicon, it shows a high temperature sensitivity of ~89 pm/℃, which is around eight times larger than the conventional FBG sensors made of silica. This facilitates the high-accuracy temperature measurement free from strain cross interference. On the other hand, the FBG is sensitive to both temperature and strain of the structure. We bonded the sensor on a cantilever beam and characterized the FBG with varying temperature without any load and varying load without changing temperature, to obtain its thermal and mechanical strain sensitivity, respectively. Using these values, we can demodulate the temperature, thermal strain and mechanical strain data from the cascaded FBG-Si FPI sensor spectrum for multiparameter measurement. The high sensitivity, enhanced resolution, and small size of the sensor make it attractive for applications where accurate measurement of strain and temperature is required. Also testing the sensor in a surface-mounted condition will render the required calibration to differentiate the thermally induced strain from mechanical strain, which is more likely to occur in practical applications.

This article is constructed as follows: Section 2 describes the fabrication method and working principle of our proposed sensor. Section 3 illustrates the experimental setup and results to characterize the sensor's performance. Section 4 emphasizes the innovation of this work by comparing with existing techniques. The conclusions of this work are provided in Section 5.

2. Sensor Fabrication and Principle

2.1 Fabrication Method

Our proposed sensor consists of an FBG inscribed in a SMF and a silicon pillar attached to the edge of this to form FP cavity. Fig. 1(a) shows a schematic of the sensor and Fig. 1(b) shows the microscopic view of the fabricated silicon FPI at the end of the fiber. For fabrication, we first write a FBG of 5 mm length and Bragg wavelength of 1549.5 nm on a coating-removed single-mode fiber following standard phase mask technology. Excimer laser (193 nm) with 500 mJ pulse energy was used to write gratings through a cylindrical lens and a phase mask. The initial reflectivity of the FBG was 92%. After fabricating the FBG, we cleaved the edge of the FBG and attached a silicon pillar of length 100 μm and diameter 150 μm to the end of it by using UV curable glue. The fabrication process of the FP interferometer is described detailed in [25]. The two parallel surfaces of the silicon pillar form the FPI.

Fig. 2 shows the reflection spectrum of the sensor at room temperature measured by an optical interrogator (Luna Hyperion Si-155), which reveals a good visibility of both the FBG peak and FP interferometric fringes. The visibility is optimized such that the FBG peak optical power is in the order of at least two times higher than the FP fringes peak intensity. This helps in signal processing to separate the FBG wavelength from the FP fringes. The free spectral range of the FP valleys is 3.3 nm, which corresponds to a cavity length of ~105 μm, consistent with the silicon pillar length.

2.2 Working Principle

The periodic wavelength λ of a FP interferometer fringe valley is as follows,

$$\lambda_{FP} = \frac{2nL}{m} \tag{1}$$

where n is the refractive index, L is the cavity length, and m is mode number. On the other hand, the Bragg wavelength of a FBG is defined as,

$$\lambda_B = 2n\Lambda \tag{2}$$

where n is the refractive index and Λ is the grating period. In both equations, the refractive index n and characteristic length (cavity length L or grating period Λ) are dependent on the surrounding perturbations, such as temperature, strain, pressure etc. and the sensitivity is dependent on the respective materials. Hence, we can simultaneously measure two different parameters if we can incorporate two different characteristic wavelengths in a single sensor structure with different sensitivities to the measurand variables. This is the main working principle for this research work, where we measure temperature and strain by monitoring two different characteristic wavelength shifts- valley wavelengths of FPI to measure temperature and Bragg wavelength of FBG for strain measurement.

2.2.1 Temperature measurement

The temperature effect on the characteristic wavelength can be described as,

$$\frac{d\lambda_n}{dT} = \lambda_n\left(\frac{1}{n}\frac{dn}{dT} + \frac{1}{L}\frac{dL}{dT}\right) \tag{3}$$

The two terms inside the parenthesis are known as thermo-optic coefficient (TOC) and thermal expansion coefficient (TEC), which are 1.5×10^{-4} RIU/°C and 2.55×10^{-6} m/(m·°C) for silicon at room temperature, much higher than silica whose TOC and TEC are 1.28×10^{-5} RIU/°C and 5.5×10^{-7} m/(m·°C) at room temperature. Assuming the refractive index of silicon and silica as 3.4 and 1.445 respectively, the temperature sensitivity according to Eq. (3) is found 72 pm/°C for silicon FPI and 14 pm/°C for silica FBG. To take advantage of high temperature sensitivity of silicon, we will use the silicon FP sensor to measure the temperature only, and the FBG will be attached to the test materials whose strain is to be measured. So experimentally the measured temperature will be as follows:

$$\Delta\lambda_{FP} = k_{FP\_T}\Delta T \qquad (4)$$

where, $\Delta\lambda_{FP}$ is the shift of average valley wavelength of the FPI sensor due to the change in temperature ΔT and k_{FP_T} is the temperature sensitivity of the FPI, whose value will be determined by a temperature calibration test in the later section.

2.2.2 Strain measurement without heat

The Bragg wavelength shift, $\Delta\lambda_B$ due to change in mechanical strain $\Delta\varepsilon_M$ is given by,

$$\Delta\lambda_B = \lambda_B(1 - p_e)\,\Delta\varepsilon_M \qquad (5)$$

where p_e is the effective strain optic constant and is given by,

$$p_e = \frac{{n_{eff}}^2}{2}(p_{12} - \sigma(p_{11} + p_{12})) \qquad (6)$$

where p_{11}, p_{12} are Pockel's constants and σ is the Poisson's ratio. For silica made fiber, the value of p_{11}, p_{12} and σ are 0.113, 0.252 and 0.16, respectively. Using these values, we can theoretically calculate the strain sensitivity of a silica made FBG as 1.2 pm/με. Experimentally we can obtain the applied strain by the following formula,

$$\Delta\lambda_{B\_\varepsilon_M} = k_{\varepsilon_M}\,\Delta\varepsilon_M \qquad (7)$$

where $\Delta\lambda_{B\_\varepsilon_M}$ is the shift in Bragg wavelength of the FBG due to change in strain $\Delta\varepsilon_M$ and k_{ε_M} is the mechanical strain sensitivity of FBG.

2.2.3 Strain measurement with heat

For an application, where both heat and strain coexist, the FBG wavelength will shift due to both thermal strain and mechanical strain. This additional thermal strain is due to the thermal expansion of the host material to which the strain sensor is attached. For this case, the total shift in FBG wavelength will be,

$$\Delta\lambda_B = \Delta\lambda_{B\_\varepsilon_T} + \Delta\lambda_{B\_\varepsilon_M} \tag{8}$$

where $\Delta\lambda_{B\_\varepsilon_T}$ is the shift due to thermal strain, which is measured from the thermal strain sensitivity ($k_{B\_\varepsilon_T}$) of FBG and measured temperature from the FPI sensor as following:

$$\Delta\lambda_{B\_\varepsilon_T} = k_{B\_\varepsilon_T}\Delta T \tag{9}$$

3. Experiment and Results

The silicon FPI is only sensitive to temperature whereas the FBG is sensitive to both temperature and strain. Therefore, we conducted separate experiments to obtain the temperature and strain sensitivity of the FPI and FBG, respectively. Then, we test the sensor for simultaneous measurements of strain and temperature to verify that the sensitivity parameters are valid in the case where both temperature and strain vary.

3.1 Temperature measurement by FPI

Fig. 3 shows the experimental setup to test the temperature sensitivity of the FPI. The sensor is placed inside of a thermal furnace and the temperature was increased from room temperature to 100 °C with an increment of 10 °C. For each temperature reading, we measured the reflection spectrum of the sensor by an optical interrogator with 1 kHz scanning rate for 10 s. For signal demodulation, we find the wavelength by Gaussian Curve fitting and taking average of multiple valleys of the FPI (details can be found in ref [25]). Fig. 4 shows the reflection spectra at different temperatures. To get a better understanding of the spectral shift, we have drawn two red arrows indicating the shift of the left most and right most valleys with temperature increase. The valleys which are affected by the FBG peak in the range of 1545-1555 nm (shown by shaded area in Fig. 4) are filtered out while measuring the average FP wavelength. We note that the FBG peak also shifted due to temperature change with a sensitivity of 11.4 pm/℃ (as indicated by the black arrow in Fig. 4). As the FBG was not bonded on any structure, the shift is purely from the thermo-optic effect and the thermal strain of the fiber. Here we only use the FPI to measure the temperature. The thermal-induced wavelength shift of the FBG and its effect on the strain measurement when the FBG is surface mounted on the structure is discussed in more detail in the following subsections.

Fig. 5(a) shows that FP average valley wavelength shifts towards the higher wavelength with increase in temperature. By linear fitting, we found the temperature sensitivity of the FPI (k_{FP_T} in Eq. 4) 89.2 pm/℃, similar to the theoretical value. The linear fitting also has a high R-square value (0.9976) which shows excellent linearity of the sensor in this temperature range. Fig. 5(b) shows the wavelength resolution of the FPI wavelength as 0.17 pm at room temperature, corresponding to a temperature resolution of 1.9×10^{-3} ℃.

3.2 Strain measurement by FBG

The FBG attached to a host structure is used to measure its strain. In case of a fixed temperature condition, the FBG will be subjected to mechanical strain only. But if there is a rise in temperature, the FBG will experience both mechanically and thermally induced strain, due to the thermal expansion of the host material it is attached to. So we conducted two separate experiments- (i) changing the load with no heat applied to obtain mechanical strain sensitivity, and (ii) changing the temperature with no load to obtain the thermally induced strain of the FBG.

3.2.1 Mechanical strain measurement

To measure the mechanical strain sensitivity, we bonded the sensor to the surface of an aluminum beam of dimension 10 cm × 2.5 cm × 0.47 cm by using an adhesive (Epoxy MS-907). It is noted that only the FBG part of the sensor was bonded on the surface of the structure, and the FPI tip was suspended in air so that it was not subjected to the applied strain (as shown in Fig. 6). The test specimen was placed in a cantilever setup, where one end of the beam was fixed to a firm support, and the other end was hanging freely where the load (weight) will be applied. Fig. 6 shows the schematic of the setup for strain measurement. For this cantilever setup, the strain ε applied to the specimen due to the load P is,

$$\varepsilon = \frac{Pxh}{2EI} \tag{10}$$

where, x is the length from the strain sensor to load, h is the thickness of the specimen, E is the Young's Modulus of the beam material (69 GPa) and I is the moment of inertia (for a rectangular beam, $I = bh^3/12$, where b and h are width and thickness of the beam).

To obtain the mechanical strain sensitivity of the FBG (k_{ε_M} in Eq. 7), we increased load from 0 to 1 kg with a step of 100 g (equivalent to 14.7 με strain) on the free hanging end of the aluminum beam in a constant temperature (22 °C). Fig. 7(a) shows the shift of the FBG peak wavelength with increasing strain. From the linear fitting, the strain sensitivity is found 1.09 pm/με, which is consistent with the theoretical value. Also, the fitting line has an excellent R-square value of 0.9998, showing good linearity of the sensor. Wavelength resolution of the FBG, obtained by taking the standard deviation of each spectral frame peak wavelength for 10s measured with a high-speed spectrometer (Model: I-Mon 256, Ibsen) at 1 kHz scanning rate is shown in Fig. 7(b), which is 0.05 pm, corresponding to a strain resolution of 0.042 με.

3.2.2 Thermally induced strain measurement

The strain measurement in the previous experiment was performed at a fixed temperature, so the FBG spectral shift was free from cross-temperature sensitivity. But if the test specimen is exposed to elevated temperature, the FBG will be subjected to both thermal and mechanical strain. To measure the sensitivity to thermal strain of the FBG sensor ($k_{B_{\varepsilon_T}}$ in Eq. 9), we placed the sensor (while it was bonded onto the surface of the aluminum beam as shown in inset of Fig. 6) inside the thermal furnace and increased temperature (no load was applied). Fig. 8 shows the shift of the FBG peak with temperature, which reveals that the bonded FBG has a sensitivity of 31.36 pm/°C. This shift resulted from the applied heat and thermally induced strain of the aluminum specimen. Theoretically, using the thermal expansion coefficient of aluminum ($23° \times 10^{-6}$m/m-K) in Eq (3), we find the thermal strain sensitivity of the sensor as 45 pm/°C. In practice, thermal strain is not fully transferred from the aluminum to the FBG due to the inefficient bonding of adhesive and other factors [26]. Nevertheless, the slope in Fig. 8 has good linearity showing a constant thermal strain transfer of the sensor at different temperatures.

3.3 Simultaneous measurement of temperature and strain

Finally, we conducted an experiment, where both temperature and strain were simultaneously varied to demonstrate how to measure these two parameters without cross-sensitivity. For this, we put the cantilever setup (as shown in Fig. 6) inside of a thermal chamber, whose temperature can be varied while we put different load on the test specimen. We measured the sensor spectrum while increasing the temperature from 30 °C to 90 °C with 10 °C increment for four different loads - 0, 250, 500 and 1000 gm (equivalent to 0, 36.65, 73.29 and 146.59 με, respectively). Fig. 9(a) and 9(b) show the shift of the FPI and FBG, respectively, for all cases. It is seen that the temperature sensitivity of the silicon FPI remained largely unchanged (89 pm/°C) regardless of the strain. This indicates that the FPI is free from strain sensitivity. On the other hand, the FBG peak wavelength shifts with a slope close to 1.10 pm/με, but the data for different loads have offsets due to the additional applied strain. For example, the inset of the Fig. 9(b) shows that at 80 °C, FBG peak wavelength increases 144 pm from no load to a load of 146.5 με. So, for simultaneous measurement, we first need to obtain the temperature data from the FPI shift, followed by measuring the strain from the FBG shift at that specific temperature.

4. Discussion

The silicon FPI-FBG sensor has several advantages for simultaneous measurement of temperature. The silicon FPI provides a strain-free high temperature sensitivity of 89 pm/℃, which is significantly higher than previously sensors with cascaded FPIs or FBGs. Also, testing the surface-bonded FBG to a host structure is more relevant to practical applications and helps to differentiate the shift induced by the mechanical strain from the one by the thermal strain. A comparison between sensors reported previously and the sensor reported here for measuring temperature and strain with respect to sensitivity is shown in Table 1:

Table 1: Comparison of existing fiber optic sensors for measuring temperature and strain

Reference	Sensor structure with working principles	Temperature and strain sensitivity	Thermal strain considered?
[5]	Single FBG, half bonded and half unbonded to host structure	10.34 pm/℃ for unbonded FBG 28.36 pm/℃ and 1.10 pm/με for bonded FBG	Yes
[6]	FBG with sawtooth stressor based on Bragg wavelength (λ_B) and birefringence induced wavelength (λ_D)	9.52 pm/℃ and 1.24 pm/με for λ_B 0.13 pm/℃ and 2.14×10^{-2} pm/με for λ_D	No
[7]	Two cascaded FBGs, one is fixed to a silica tube and another is loosely bonded	15.7 pm/℃ and 5.46 pm/με	No

[8]	Cascaded FPI sensors by air and silica cavity	0.902 pm/°C and 2.97 pm/με for air cavities, 10.45 pm/°C and 2.8 pm/με for silica cavities	No
[9]	Two FPI formed by Grading index few mode fibers	10.81pm/°C and 1.03pm/με for high freq FP 0 and 2.72 pm/με for low freq FP	No
[15]	Micro-tapered fiber grating based on wavelength and transmission change	49.6 pm/°C -0.55 pm/με	No
[22]	Air cavity FPI and FBG	0.5 pm/°C and 5.34 pm/με for FP 15pm/°C and 1.71 pm/με for FBG	No
[23]	FBG and air cavity FP	11.7pm/°C and 1.2 pm/με for FBG -0.1mrad/°C and -0.9 mrad/με for FP	No
[24]	Regenerated grating (RG) and FPI (SMF-HCF-SMF)	13.97pm/°C and 1.063 pm/με for RG 0.82pm/°C and 1.23 pm/με for FPI	No
This article	Silicon FPI-FBG	89 pm/°C for FPI 31.37 pm/°C for FBG (thermal strain) 1.09 pm/με for FBG (mechanical strain)	Yes

Here, it needs to be mentioned that the strain sensitivity of the FBG is not constant over a broad temperature range. We used a constant value for aluminum's Young's modulus (69 GPa) when converting from load to strain in Eq. 10. But in practice, Young's modulus for any materials changes with temperature. Especially at an elevated temperature, the reduced value of Young's modulus needs to be considered for accurate strain measurement. Also, the epoxy bonding strength may change at higher temperature, which needs to be calibrated as well. Since these two factors vary with host materials and epoxy used in the test, we did not elaborate on the calibration of Young's modulus and strain transfer efficiency for higher temperature.

5. Conclusion

We reported a novel sensor for simultaneous measurement of temperature and strain composed of a FBG and silicon FPI. The sensor provides high temperature sensitivity of 89 pm/°C, unaffected by strain, thanks to the high thermal expansion and thermo-optic coefficient of silicon. The FBG's strain sensitivity is characterized for both cases, with and without heat. The effect of thermal expansion of the host material is demonstrated for accurate strain measurement. Experimental results show that the FBG strain sensitivity is 1.09 pm/με, consistent with the theory and the thermal expansion of host structure results in 32 pm/℃ shift for FBG. Finally, a simultaneous test has been conducted to verify that the temperature and strain sensitivity holds up to 90 ℃ temperature and 150 με strain. The sensitivity needs to be calibrated for different host structure, and epoxy as the Young's modulus and thermal expansion coefficient vary materials to materials.

Code, Data, and Materials Availability

Data underlying the results presented in this paper are not publicly available at this time but may be obtained from the author upon reasonable request.

Acknowledgments

This material is based upon work supported by the National Science Foundation under Grant No. 1918074 and by the U.S. Department of Energy under Grant No. DE-FE0031899.

References

1. Rocha H, Semprimoschnig C, Nunes JP. Sensors for process and structural health monitoring of aerospace composites: A review. *Eng Struct*. 2021;237(January). doi:10.1016/j.engstruct.2021.112231
2. Liu T, Liu L, Gou GY, et al. Recent Advancements in Physiological, Biochemical, and Multimodal Sensors Based on Flexible Substrates: Strategies, Technologies, and Integrations. *ACS Appl Mater Interfaces*. 2023;15(18):21721-21745. doi:10.1021/acsami.3c02690
3. Watson J, Castro G. A review of high-temperature electronics technology and applications. *J*

Mater Sci Mater Electron. 2015;26(12):9226-9235. doi:10.1007/s10854-015-3459-4

4. Ramakrishnan M, Rajan G, Semenova Y, Farrell G. Overview of fiber optic sensor technologies for strain/temperature sensing applications in composite materials. *Sensors*. 2016;16(1). doi:10.3390/s16010099
5. Her SC, Lin WN. Simultaneous measurement of temperature and mechanical strain using a fiber Bragg grating sensor. *Sensors*. 2020;20(15). doi:10.3390/s20154223
6. Guo K, He J, Shao L, Xu G, Wang Y. Simultaneous Measurement of Strain and Temperature by a Sawtooth Stressor-Assisted Highly Birefringent Fiber Bragg Grating. *J Light Technol*. 2019;38(7):2060-2066. doi:10.1109/JLT.2019.2959671
7. Tian Q, Xin G, Lim K, et al. Optical Fiber Sensor With Double Tubes for Accurate Strain and Temperature Measurement Under High Temperature up to 1000 ◦C. *IEEE Sens J*. 2022;22(12):11710-11716. doi:10.1109/JSEN.2022.3167950
8. Tian J, Jiao Y, Ji S, Dong X, Yao Y. Cascaded-cavity Fabry–Perot interferometer for simultaneous measurement of temperature and strain with cross-sensitivity compensation. *Opt Commun*. 2018;412(November 2017):121-126. doi:10.1016/j.optcom.2017.12.005
9. Fu X, Liu L, Ma S, Fu G, Jin W, Bi W. Dual-parameter four-beam interferometric sensor for the measurement of temperature and strain with a double air-gaps structure based on graded-index few mode fiber. *OSA Contin*. 2019;2(12):3381-3392. doi:10.1364/OSAC.2.003381
10. Weng Y, Ip E, Pan Z, Wang T. Single-end simultaneous temperature and strain sensing techniques based on Brillouin optical time domain reflectometry in few-mode fibers. *Opt Express*. 2015;23(7):1053-1059. doi:10.1364/OE.23.009024
11. Alahbabi M, Cho YT, Newson TP. Comparison of the methods for discriminating temperature and strain in spontaneous Brillouin-based distributed sensors. *Opt Lett*. 2004;29(1):26-31. doi:10.1364/OL.29.000026
12. Ghimire M, Wang C. Highly sensitive fiber loop ringdown strain sensor with low temperature sensitivity. *Meas Sci Technol*. 2017;28(10). doi:10.1088/1361-6501/aa82a3

13. Li R, Tian C, Zhang Y, Zhang J, Chen X, Liu S. Simultaneous Measurement of Force and Temperature by a Multi-Position Fiber Loop Ringdown Sensor Array. *J Light Technol*. 2015;33(17):3607-3612. doi:10.1109/JLT.2015.2446652

14. Jin W, Michie WC, Thursby G, Konstantaki M, Culshaw B. Simultaneous measurement of strain and temperature: error analysis. *Opt Eng*. 1997;36(2):598-602. doi:10.1117/1.601233

15. Yoon MS, Park S, Han YG. Simultaneous measurement of strain and temperature by using a micro-tapered fiber grating. *J Light Technol*. 2012;30(8):1156-1160. doi:10.1109/JLT.2011.2170552

16. Gomes AD, Ferreira MS, Bierlich J, et al. Optical Harmonic Vernier Effect : A New Tool for High Performance Interferometric Fibre Sensors. *Sensors*. 2019;19(Art. 5431). doi:10.3390/s19245431

17. Paixão T, Araújo F, Antunes P. Highly sensitive fiber optic temperature and strain sensor based on an intrinsic Fabry–Perot interferometer fabricated by a femtosecond laser. *Opt Lett*. 2019;44(19):4833. doi:10.1364/ol.44.004833

18. Hou L, Zhao Ch, Xu B, Mao B, Shen C, Wang DN. Highly sensitive PDMS-filled Fabry – Perot interferometer temperature sensor based on the Vernier effect. *Appl Opt*. 2019;58(18):4858-4865. doi:10.1364/AO.58.004858

19. Huang H, Chen H, Jiang C, Guo X, Sun S. Simultaneous measurement of gas pressure and temperature based on Fabry-Pérot cavity cascading fiber Bragg grating. *AIP Adv*. 2021;11(12). doi:10.1063/5.0067521

20. Chen LX, Huang XG, Li JY, Zhong ZB. Simultaneous measurement of refractive index and temperature by integrating an external Fabry-Perot cavity with a fiber Bragg grating. *Rev Sci Instrum*. 2012;83. doi:10.1063/1.4721274

21. Zhao Y, Lv R-Q, Wang D, Wang Q. Fiber Optic Fabry-Perot Magnetic Field Sensor with Temperature Compensation Using a Fiber Bragg Grating. *IEEE Trans Instrum Meas*. 2014;63(9):2210-2214. doi:10.1109/TIM.2014.2308360

22. Yang T, He X, Ran Z, et al. Highly integrated all-fiber FP/FBG sensor for accurate measurement

of strain under high temperature. *Materials (Basel)*. 2018;11. doi:10.3390/ma11101867

23. Liu Q, Ran ZL, Rao YJ, Luo SC, Yang HQ, Huang Y. Highly Integrated FP/FBG Sensor for Simultaneous Measurement of High Temperature and Strain. *IEEE Photonics Technol Lett*. 2014;26(17):1715-1717. doi:10.1109/LPT.2014.2331359

24. Liu H, Yang HZ, Qiao XG, et al. Strain measurement at high temperature environment based on Fabry-Perot interferometer cascaded fiber regeneration grating. *Sensors Actuators, A Phys*. 2016;248:199-205. doi:10.1016/j.sna.2016.07.028

25. Liu G, Han M, Hou W. High-resolution and fast-response fiber-optic temperature sensor using silicon Fabry-Pérot cavity. *Opt Express*. 2015;23(6):7237. doi:10.1364/oe.23.007237

26. Liang M, Chen N, Fang X, Wu G. Strain transferring mechanism analysis of the surface-bonded FBG sensor. *Appl Opt*. 2018;57(20):5837-5843. doi:10.1364/AO.57.005837

Hasanur R. Chowdhury is a research scientist at Nusenics in Michigan, USA. He received his BS and MS degrees in Electrical and Electronic Engineering from the University of Dhaka, Bangladesh, in 2016 and 2018, respectively, and his PhD degree in Electrical Engineering from Michigan State University, USA, in 2023. His research interests include the characterization and development of fiber-optic devices and systems.

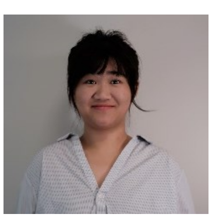

Xiaoli Wang is a Ph.D. student at Electrical and Computer Engineering Dept. in Michigan State University, USA. She received her BS degree from Northeastern University (Shenyang, China) in Electrical and Electronic Engineering and her MS degree in Physics Engineering from University of Chinese Academy of Sciences (Beijing, China), in 2017 and 2021, respectively. Her research directions include the fiber-optic bolometer characterization and temperature sensor development with high resolution and fast response.

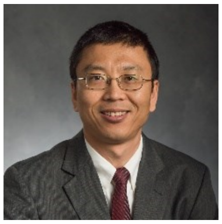

Ming Han is a Fellow of SPIE. He received his B.S. degrees in electronic engineering from Tsinghua University, Beijing, China, in 1998 and his Ph.D. degree in electrical engineering from the Virginia Polytechnic Institute and State University (Virginia Tech), Blacksburg, VA, USA, in 2006. He is a Professor with the Department of Electrical and Computer Engineering, Michigan State University, East Lansing, MI, USA. He is the founder and President of Nusenics, LLC, Okemos, MI, USA. His research interests include fiber-optic sensors and sensor instrumentation. He is an Topical Editor of *Optics Letters*.

Caption List

Fig. 1 (a). Sensor Schematic Diagram, (b) microscopic view of the silicon FPI.

Fig. 2 Reflection spectrum of the FBG-FPI sensor at room temperature.

Fig. 3 Experimental setup for temperature test by FPI.

Fig. 4 Reflection spectra at various temperatures. The two red arrows indicate the shift of the left most and right most valley. Grey shaded valleys are affected by FBG shift, hence are filtered out for average wavelength measurement.

Fig. 5 (a) Wavelength shift of the FP valleys with temperature, (b) wavelength resolution measured over 10s.

Fig. 6 Experimental setup for strain measurement. Inset shows the details of sensor installation.

Fig. 7 (a) Wavelength shift of the FBG peak with strain, (b) wavelength resolution of the FBG peak at initial condition.

Fig. 8 Shift of the FBG peak wavelength with temperature as bonded with aluminum beam.

Fig. 9 (a) FPI and (b) FBG wavelength shift with temperature with and without load (strain).

Table 1: Comparison of existing fiber optic sensors for measuring temperature and strain